Electrochimica Acta 53 (2008) 5517–5522

Contents lists available at ScienceDirect

Electrochimica Acta

journal homepage: www.elsevier.com/locate/electacta

Water and methanol crossover in direct methanol fuel cells—Effect of anode diffusion media

Fuqiang Liu[1], Chao-Yang Wang*

Departments of Materials Science and Engineering, and Mechanical and Nuclear Engineering, and Electrochemical Engine Center (ECEC), The Pennsylvania State University, University Park, PA 16802, United States

ARTICLE INFO

Article history:
Received 13 February 2008
Received in revised form 3 March 2008
Accepted 4 March 2008
Available online 13 March 2008

Keywords:
Direct methanol fuel cell
Anode microporous layer
Water crossover
Methanol crossover

ABSTRACT

Various anode diffusion media have been experimentally studied to reduce water crossover in a direct methanol fuel cell (DMFC). A two-phase water transport model was also employed to theoretically study their effects on water transport and saturation level in a DMFC anode. It is found that wettability of the anode microporous layer (MPL) has a dramatic effect on water crossover or the water transport coefficient (α) through the membrane. Under different current densities, the MEA with a hydrophobic anode MPL has consistently low α, several times smaller than those with a hydrophilic MPL or without an anode MPL. Methanol transport in the anode is found to be not influenced by a hydrophobic anode MPL but inhibited by a hydrophilic one. Constant-current discharge shows that the MEA with hydrophobic anode MPL displays much smaller voltage fluctuation than that with the hydrophilic one. A modeling study of anode water transport reveals that the liquid saturation in the anode is lowered significantly with the increase of anode MPL contact angle, which is thus identified as a key parameter to minimize water crossover in a DMFC.

1. Introduction

Direct methanol fuel cells (DMFCs) are attractive power sources for portable electronics, in part because of their high energy density and easy storage of liquid fuel [1]. Work in our laboratory has demonstrated the paramount importance of water crossover through the membrane in the development of high concentration methanol fuel cells with high performance [2,3]. We first revealed the direct link between the water transport coefficient (α) through the membrane and maximum methanol concentration possibly used in the anode feed and thus proposed the development of low-α membrane-electrode assembly (MEA) [2,3]. Here α is defined as the ratio of the net water flux through a membrane to the protonic flux. The α value for conventional DMFCs based on Nafion 117 is roughly 2.5 [4], which corresponds to a theoretical maximum methanol concentration of ~3 M, thus dramatically limiting the energy density of a DMFC system. On the other hand, 10 M methanol operation requires an MEA to have α equal to or smaller than 0.6. To enable direct use of pure methanol, α must be reduced to below zero [3]. High power direct methanol fuel cells running on 15 M to neat methanol have been successfully demonstrated by Wang et al. [5,6], attributed to a minimized or even negative water crossover.

In our prior publications [2,3] we have experimentally achieved $\alpha \sim 0.6$ at 60 °C, using dry air at atmospheric pressure, and under typical cathode flow conditions. Since then, there has been extensive follow-up work and the importance of water crossover has become a consensus in the DMFC community for portable power applications [7–9]. However, all subsequent work cannot reach the same low level of α as originally demonstrated in [2,3]. The present paper will explain why there exists such a gap. We shall also reveal, for the first time, that the anode microporous layer (MPL) is a more influential factor in reducing water crossover through the membrane in DMFCs than the cathode MPL. Previously, all the literature has emphasized exclusively the important role of a cathode MPL in returning water from the cathode to anode thus leading to low α [2,3,7–13], following the capillary flow theory of Pasaogullari and Wang [14].

In this work we report on experimental data and theoretical analysis showing that the anode MPL is a more important factor than the cathode MPL for minimizing water crossover through the membrane in DMFCs. A more expanded version of the present paper can be found in the Ph.D. thesis of Liu [6].

2. Experimental

Both MEA fabrication and experimental hardware have been detailed in previous publications [2,3] and thus are not repeated here. The cathode gas diffusion layer (GDL) is carbon cloth with a pre-coated hydrophobic MPL containing carbon black and PTFE.

* Corresponding author. Tel.: +1 814 863 4762; fax: +1 814 863 4848.
E-mail address: cxw31@psu.edu (C.-Y. Wang).
[1] Present address: United Technologies Research Center, East Hartford, CT 06108, United States.

0013-4686/$ – see front matter © 2008 Elsevier Ltd. All rights reserved.
doi:10.1016/j.electacta.2008.03.011

Carbon papers with 10% wet-proofing (Toray TGPH 090) were used as the anode diffusion medium (DM) substrate. A mixture of Vulcan XC72R carbon black and 40 wt% PTFE (TFE 30, Dupont) or Nafion was coated on the carbon paper using a gap-adjustable blade to fabricate either a hydrophobic or a hydrophilic MPL with the same loading of 2 mg/cm^2 (carbon and binder). In this work, the anode DM is generally referred to as the carbon paper substrate either with or without a MPL. MEAs of 12 cm^2 based on Nafion 112 membranes were prepared by the decal method. The catalyst loadings in the anode and cathode catalyst layer (CL) were 5.3 mg PtRu/cm^2 and 1.2 mg Pt/cm^2, respectively.

To investigate the surface morphologies of different diffusion media, scanning electron microscopy (SEM, Philips XL20) was used. Fresh samples of different anode diffusion media were examined at relatively small magnification to reveal porosity and surface structure.

The MEAs were mounted between two identical graphite flow plates with two-pass serpentine channels. The cell was operated at 60 °C and ambient pressure on both sides. 2 M methanol solution (0.19 mL/min) and dry air (97.3 mL/min) were fed to the anode and cathode, corresponding to stoichiometries of 2 and 3 at 150 mA/cm^2, respectively. The total water collected from the cathode exit at constant-current discharge, after correcting for the water produced from oxidation of the crossover methanol, was used to calculate the net water transport coefficient, α.

3. Liquid water transport in the DMFC anode

The multiphase mixture (M^2) model is used to simulate two-phase water transport in the anode. Considering 1D water transport along the thickness, the governing equation in both carbon paper and MPL is written as [14]

$$\frac{\mathrm{d}}{\mathrm{d}x}(\gamma_c u C^{H_2O}) + \frac{\mathrm{d}}{\mathrm{d}x}\left[\left(\frac{1 - C_l^{MeOH} M^{MeOH}/\rho_l}{M^{H_2O}} - \frac{C_{sat}^{H_2O}}{\rho_g}\right) j_l\right] = 0 \quad (1)$$

The two terms at the left-hand side describe water transport by convection and capillary transport, respectively. Here, $C_l^{MeOH} M^{MeOH}/\rho_l$ is the mass fraction of methanol in the liquid, assuming a uniform methanol concentration everywhere in the diffusion media, and γ_c is the advection factor. The advection factor is expressed as

$$\gamma_c = \frac{\rho}{C^{H_2O}}\left(\frac{\lambda_l}{M^{H_2O}} + \lambda_g \frac{C_{sat}^{H_2O}}{\rho_g}\right) \quad (2)$$

where ρ, λ_l and λ_g are the two-phase mixture density, relative mobility of liquid and gas phases, respectively

$$\lambda_l = \frac{k_{rl}/\nu_l}{(k_{rl}/\nu_l) + (k_{rg}/\nu_g)}, \quad \lambda_g = 1 - \lambda_l \quad (3)$$

where k_{rg} and k_{rl} are the relative permeabilities of individual phases, which are equal to the cube of phase saturations. The total water concentration is expressed in terms of liquid saturation, s, as

$$C^{H_2O} = s C_l^{H_2O} + (1 - s) C_{sat}^{H_2O} \quad (4)$$

In Eq. (1), j_l is the liquid flux driven by capillary pressure gradient [15–17]

$$j_l = \frac{\lambda_l \lambda_g \rho K}{\mu}\frac{\mathrm{d}}{\mathrm{d}x}\left(\sigma \cos(\theta_C)\left(\frac{\varepsilon}{K}\right)^{1/2} J(s)\right) \quad (5)$$

where $J(S)$ is the Leverett function and is given for both hydrophilic and hydrophobic media as [14]

$$J(s) = \begin{cases} 1.417(1-s) - 2.120(1-s)^2 + 1.263(1-s)^3, & \text{if } \theta_c < 90^\circ \\ 1.417s - 2.120s^2 + 1.263s^3, & \text{if } \theta_c > 90^\circ \end{cases} \quad (6)$$

where θ_c is the contact angle.

Integration of Eq. (1) over the diffusion medium thickness yields

$$\gamma_c u C^{H_2O} + \left(\frac{1 - C_l^{MeOH} M^{MeOH}/\rho}{M^{H_2O}} - \frac{C_{sat}^{H_2O}}{\rho_g}\right) j_l = \frac{I}{6F}(1 + 6\alpha) \quad (7)$$

Superficial velocities in the above equation at the two interfaces are calculated as

$$u = \frac{j_m}{\rho} = \frac{1}{\rho}\left[\frac{I}{6F}(1 + 6\alpha) M^{H_2O} + \frac{I}{6F} M^{MeOH} - \frac{I}{6F} M^{CO_2}\right] \quad (8)$$

where j_m is the total mass flux through the interface in both phases. Expression of other parameters can be found in Table 2 and refs. [14,18]. Now Eq. (7) can be rewritten using s as the primary variable. The liquid saturation profiles in the anode DM and MPL can thus be obtained using a fourth-order Runge-Kutta method.

At small anode stoichiometry, water saturation at the anode GDL/channel interface is expected to be less than 100%, since CO_2 bubbles cannot be removed completely from the surface of the anode diffusion medium. We assume the liquid saturation at the anode DM/channel interface arbitrarily to be 65%. The liquid saturation at the DM/MPL interface in the MPL can be calculated by assuming continuous gas and liquid pressures across that interface [19], i.e.,

$$p_c^{GDL}\big|_{GDL-MPL_{int}} = p_c^{MPL}\big|_{GDL-MPL_{int}} \quad (9)$$

The different properties of the two layers cause a discontinuity in liquid saturation across the interface.

While the above-described model is simplified, it is intended to qualitatively explain the dramatic effect of anode diffusion media. A more sophisticated two-phase model aimed at the quantitative prediction of cell performance and water/methanol transport in a DMFC is available in refs. [20,21].

4. Results and discussion

We are interested primarily in how the structure and wettability of anode diffusion media yield low α. To ascertain the effect of anode MPL, three anode diffusion media are investigated in this study, with details listed in Table 1. Carbon paper, carbon paper with a hydrophilic MPL and with a hydrophobic MPL are employed in MEA-1, MEA-2, and MEA-3, respectively. SEM images of their

Table 1
Electrochemical performance parameters of MEAs using different anode diffusion media

Sample	Anode diffusion medium	HFR (Ω cm^2)	MeOH crossover at open circuit, $I_{c,oc}$ (mA/cm^2)	Average cell voltage at 150 mA/cm^2 (V)	α value at 150 mA/cm^2
MEA-1	C paper w/anode MPL (aMPL)	0.190	257	0.379	1.153
MEA-2	C paper w/hydrophilic aMPL	0.183	223	0.328	1.743
MEA-3	C paper w/hydrophobic aMPL	0.212	242	0.398	0.335
MEA-4	C paper w/two-layer MPL	0.218	240	0.387	0.312
MEA-5	Carbon paper w/higher PTFE fraction (60%) in aMPL	0.191	237	0.379	0.302

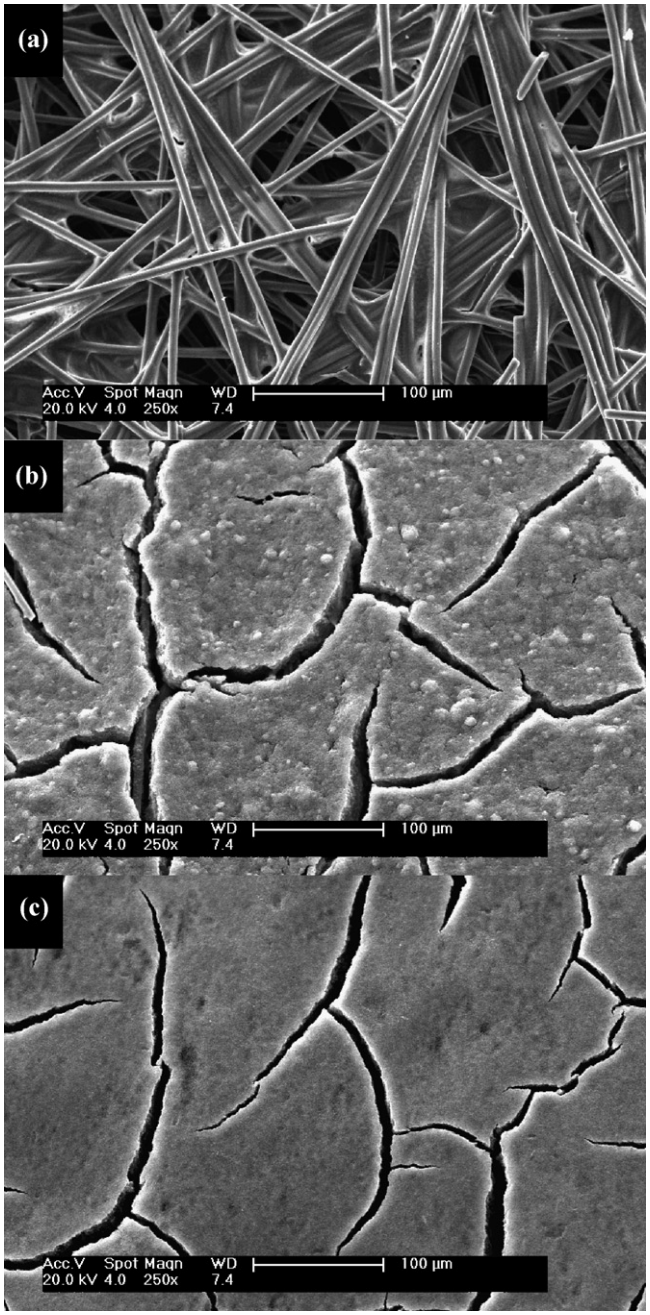

Fig. 1. Surface morphologies of various anode diffusion media: (a) 10% wet-proofing Toray carbon paper (TGPH-090), (b) hydrophilic MPL (40% Nafion), and (c) hydrophobic MPL (40% PTFE).

surfaces are shown in Fig. 1. Carbon paper is a microscopically complex fibrous structure with the pore size distribution ranging from a few microns to tens of microns. MPLs have much smaller pore sizes (~100 nm), with uniform cracks (mud cracking), induced by volume shrinkage of carbon/PTFE (or carbon/Nafion) slurry during annealing. Although it is difficult to find any noticeable structural difference in the two MPLs from the SEM images, it is assumed that the pore size and porosity in the hydrophilic MPL would decrease due to swelling and expansion of ionomer upon full hydration; while those of hydrophobic MPL remain the same. Differences in porosity, permeability, pore size distribution, surface wettability, and liquid retention of the three diffusion media would result in different two-phase flow and water transport characteristics [22].

Table 2
Parameters used in analysis

Parameters	Value
Liquid surface tension (60 °C), σ (N/m)	0.07
Density of 2 M liquid methanol solution, ρ_l (kg/m^3)	988.2
Liquid kinematic viscosity, ν_l (m^2/s)	7.10×10^{-6}
Gas kinematic viscosity, ν_g (m^2/s)	3.06×10^{-4}
Density of saturated vapor, ρ_g (kg/m^3)	0.977
Saturated water vapor molar concentration, $C_{sat}^{H_2O}$ (mol/m^3)	7.20
Methanol concentration in GDL, C_l^{MeOH} (mol/m^3)	2000
GDL permeability, K_{GDL} (m^2)	1.0×10^{-13}
GDL thickness, ΔX_{GDL} (μm)	260
Contact angle of GDL, θ_{GDL} (°)	100
Porosity of the GDL, ε_{GDL}	0.45
MPL permeability, K_{GDL} (m^2)	7.0×10^{-15}
MPL thickness, ΔX_{GDL} (μm)	30
Contact angle of hydrophobic MPL, θ_{GDL} (°)	100
Porosity of hydrophobic MPL, ε_{GDL}	0.2
Contact angle of hydrophilic MPL, θ_{GDL} (°)	30
Porosity of hydrophilic MPL, ε_{GDL}	0.2

The quick-scan DMFC polarization curves of the three MEAs are shown in Fig. 2. The limiting current densities of MEA-1 and MEA-3 are almost identical, approximately 50 mA/cm^2 larger than that of MEA-2. At 150 mA/cm^2, the two MEAs have cell voltages about 25 mV higher than that of MEA-2. The performance curves of the three MEAs are consistent with their anode polarizations as shown in Fig. 3. MEA-2 has the smallest anode limiting current density, around 300 mA/cm^2, which is roughly 50 mA/cm^2 smaller than those of MEA-1 and MEA-3. This indicates that methanol transport in the anode is barely influenced by a hydrophobic MPL, but is inhibited by a hydrophilic MPL, due to the reduced porosity by ionomer hydration and expansion. This is probably the reason why MEA-1 and MEA-3 show smaller methanol oxidation overpotential than that of MEA-2 when the current density is beyond ~100 mA/cm^2.

The high-frequency resistance (HFR) and methanol crossover at open circuit are also shown in Table 1 for the three MEAs. HFR is taken as the value where AC impedance spectra intercept with the real axis. The hydrophilic MPL has the smallest HFR and methanol crossover, i.e. 0.183 Ω cm^2 and 223 mA/cm^2, respectively.

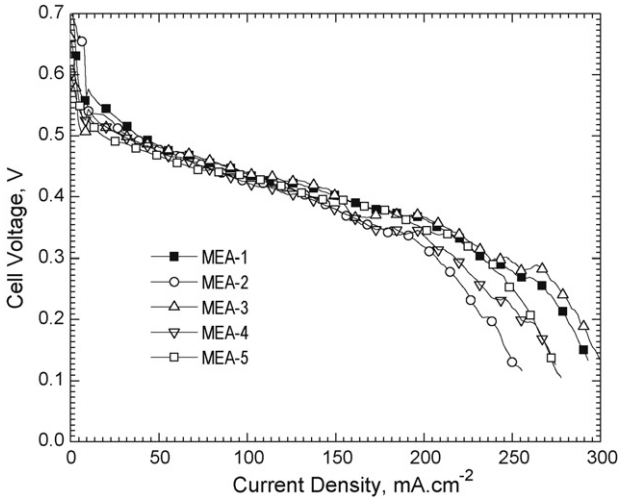

Fig. 2. Quick-scan DMFC polarization curves of MEAs with different anode diffusion media. Carbon cloth with MPL as the cathode diffusion medium and Nafion 112 were employed. The cell is operated at 60 °C, with flow rates of 2 M methanol solution and dry air at 0.19 and 97.3 mL/min, corresponding to 2 and 3 at 150 mA/cm2, respectively.

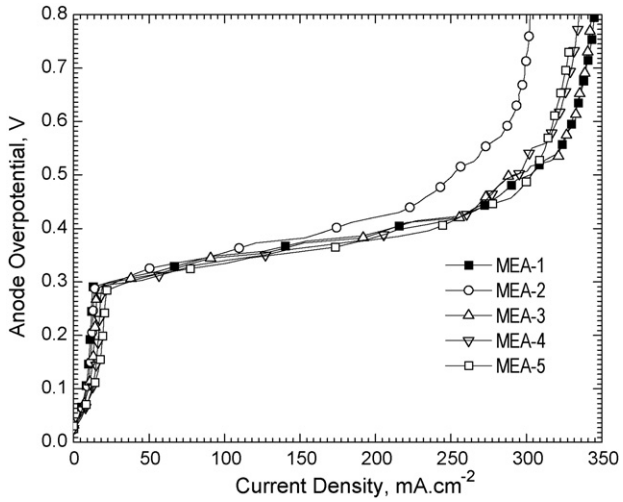

Fig. 3. Quick-scan anode polarization curves of MEAs with different anode diffusion media.

This probably originates from good contact between the carbon paper backing and anode catalyst layer via a compact hydrophilic MPL using Nafion ionomer as the binder. It also gives the lowest methanol crossover rate, consistent with its smallest anode limiting current density. MEA-3 with a hydrophobic MPL has slightly higher HFR and methanol crossover, and MEA-1 without anode MPL has the largest methanol crossover.

Constant-current discharge of these MEAs at various current densities was performed at 60 °C and ambient pressure on both sides. DMFC voltage variations over discharge time at 150 mA/cm^2 are recorded in Fig. 4. The average cell voltage during constant-current discharge is 0.398 V for MEA-3, much higher than 0.328 V of MEA-2 and 0.379 V of MEA-1. It is interesting to note from Fig. 4 that MEA-1 and MEA-3 operate more stably than MEA-2, which shows large voltage fluctuations during constant-current discharge. These fluctuations are believed to be caused by liquid water accumulation and subsequent removal in the cathode GDL and channels [23], corresponding to slow voltage decay and sudden recovery, as confirmed by experiments with increased cathode stoichiometry (results not shown here). During constant-current discharge at 150 mA/cm^2, the water collected from the cathode outlet stream was used to calculate α values, which are listed in Table 1. The anode MPL wettability has a dramatic effect on water transport in DMFCs. The α values of the MEAs with hydrophobic and hydrophilic MPLs are 0.335 and 1.743, respectively; MEA-1 without anode MPL has α value right between these two cases. Recall the definition of α, higher value means larger amount of water transported from the anode through the membrane to the cathode; thus, the transported water plus the product water from oxygen reduction would easily flood the cathode. This is the reason why MEA-2 displays so large cell voltage fluctuation during constant-current discharge.

The large disparity in α between the cases with and without an anode MPL as shown in Table 1 explains why the later works of [7–9], without using the anode MPL, were not able to reproduce the low level of water crossover as reported in the original work of [2,3].

To investigate more clearly the effect of anode diffusion medium properties on water transport in DMFCs, α values are measured for a range of current densities and plotted in Fig. 5. For all MEAs, α values initially decrease dramatically with current densities and then diminish gradually when current densities are beyond 100 mA/cm^2. This clearly indicates that the driving force for water back flow is current-dependant and increases dramatically with the current as the cathode accumulates more water and the anode becomes more gaseous. Another significant feature is that the hydrophobic anode MPL has consistently lower α than the hydrophilic one over the whole spectrum of current density. For example, at 150 mA/cm^2, α value for the hydrophobic MPL is about 1/5 of the hydrophilic one! This surprising result offers a new way to reduce α using a hydrophobic anode MPL.

The hydrophobic and hydrophilic MPLs studied in the present work create dramatically different situations of liquid water

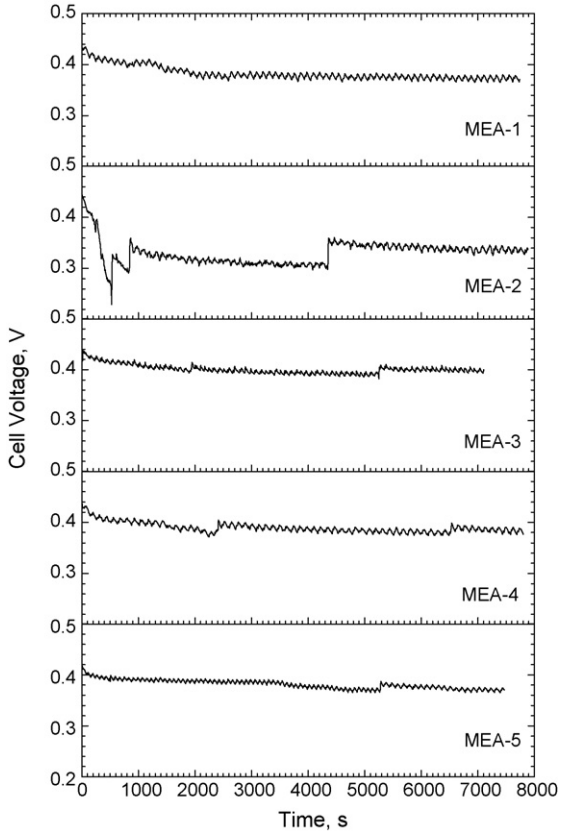

Fig. 4. DMFC voltage variations with time at constant-current discharge (150 mA/cm^2) for different MEAs with different anode diffusion media.

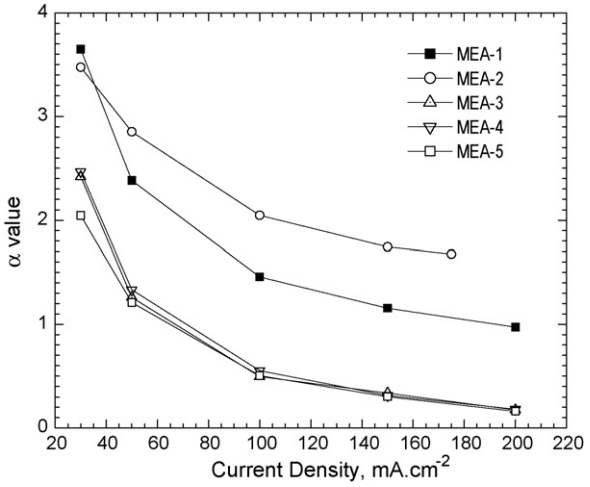

Fig. 5. Net water transport coefficients (α) across the membrane for different MEAs. α values shown in the figure exclude the water produced by oxidation of crossover methanol on the cathode.

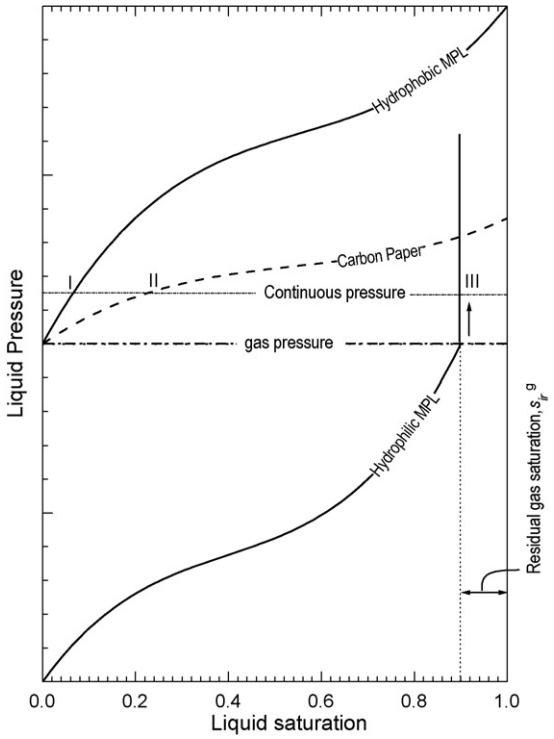

Fig. 6. Schematic illustration of liquid-phase pressure profiles in different diffusion media. The dotted line is a hypothesized line, indicating a continuous pressure at the interface between different diffusion media. The three points I, II, and III indicate the liquid saturations in carbon paper, hydrophobic MPL, and hydrophilic MPL, respectively.

transport and thus water saturation in the porous anode. The liquid-phase transport in porous media is governed by a gradient in capillary pressure (wicking action), which is defined as the difference between gas-phase and liquid-phase pressures. In hydrophobic diffusion media, the capillary pressure is negative, hence the liquid pressure is larger than the gas-phase pressure, whereas in hydrophilic media, the gas-phase pressure is higher than that of the liquid phase [15]. When two diffusion media with differing wettability are in contact with each other, the liquid pressure difference between the hydrophobic and hydrophilic media always pushes liquid water from the former into the latter, rendering the latter fully saturated and the former largely unsaturated, as schematically shown in Fig. 6. For all diffusion media, the capillary pressure increases with the liquid saturation. At the MPL/DM interface, if a continuous liquid pressure is assumed (shown as a dotted line in the figure), the capillary pressure would push liquid water into the hydrophilic MPL. Eventually, no more gas phase will be displaced by the liquid phase, even with further increases in capillary pressure (as indicated by an arrow in the figure); therefore, a residual or irreducible gas saturation [14], s_{ir}^g (=0.1), is assumed. The three points I, II, and III in Fig. 6 denotes the liquid saturations in hydrophobic MPL, carbon paper, and hydrophilic MPL, respectively, under that continuous pressure. Clearly, the hydrophobic MPL exhibits much lower anode water saturation than the hydrophilic MPL or carbon paper without MPL.

Fig. 7 shows the calculated water saturation profiles in the three anode diffusion media. The thickness of carbon paper is 260 μm, and both hydrophilic and hydrophobic MPLs have the same thickness of 30 μm. There are three important interfaces in the DMFC anode: (1) DM/channel interface, where the liquid saturation is assumed to be 0.65, which is a reasonable assumption because of the gaseous nature of DMFC anode due to CO_2 evolution; (2) DM/MPL interface, where a saturation jump is expected due to a

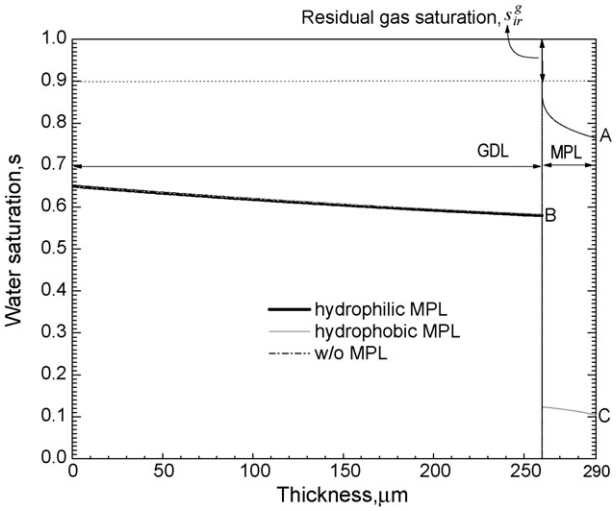

Fig. 7. Calculated liquid water saturation profiles in three different anode diffusion media. A, B, and C in the figure indicate water saturation levels at the anode catalyst layer interface for hydrophilic MPL, w/o MPL, and hydrophobic MPL, respectively. α values used in these calculations are obtained from experimental measurements.

continuous liquid pressure; and (3) MPL/anode CL interface, where the water saturation determines the water back-transport and hence α value. In Fig. 7A–C correspond to liquid saturations at the anode CL surface for the three anode diffusion media: hydrophilic MPL, carbon paper without MPL, and hydrophobic MPL, respectively. In the carbon paper DM, the saturation decreases almost linearly, from 0.65 at the DM/channel interface to 0.58 at DM/MPL interface (point B). At this point, it rises to $(1 - s_{ir}^g)$ (i.e. the maximum liquid saturation possible) in the hydrophilic MPL and it reduces to around 0.13 in the hydrophobic MPL. The water saturation decreases in both MPLs, and eventually reaches 0.76 (point A) and 0.1 (point C) at the anode CL surface for the hydrophilic and hydrophobic MPLs, respectively.

The reason that MEA-3 with hydrophobic anode MPL shows the lowest α is related to its ability to depress the anode liquid water saturation and enhance the water content gradient across the membrane. The water back transport under this gradient yields the very low α of MEA-3. On the contrary, the MEAs with hydrophilic or without anode MPL have relatively smaller water content gradient across the membrane, thus higher α.

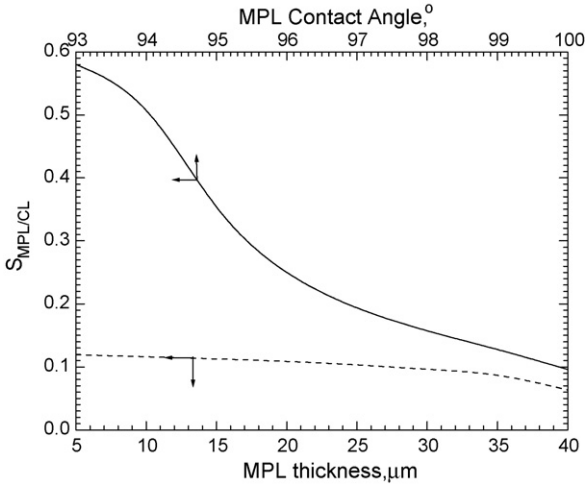

Fig. 8. Influence of hydrophobic MPL thickness and contact angle on water saturation at the interface of anode catalyst layer/MPL.

The hydrophobicity (contact angle) and thickness of the hydrophobic MPL are numerically explored to further reduce the water crossover in DMFCs. Variations of liquid water saturation at the hydrophobic MPL/anode CL interface with MPL contact angle and thickness are shown in Fig. 8. MPL thickness has a marginal effect on liquid saturation at the anode CL surface. The water saturation is almost independent of the thickness until 35 μm, beyond which saturation slowly decreases with the thickness. Contact angle of anode MPL, however, seems to have a dramatic effect on liquid saturation, which decreases steeply from ∼0.6 at 93° to ∼0.1 at 100°.

Increasing the MPL contact angle or making the MPL more hydrophobic appears more effective to reduce α than using a thicker MPL. To evaluate the calculated results, two additional MEAs, MEA-4 with double-layer MPL and MEA-5 with higher PTFE fraction (60 wt%) in the MPL, were fabricated and tested. The purpose of using higher PTFE fraction is to increase the MPL contact angle. From Table 1, the two MEAs seem to have no significant influence on cell resistance and methanol crossover, which are all comparable to that of MEA-3 with a single-layer MPL. However, the limiting current densities of the two MEAs are 20–30 mA/cm^2 smaller than that of MEA-3, as indicated in the anode polarizations in Fig. 3. This can be easily explained by increased methanol transport resistance due to either additional diffusion length of thicker MPL or reduced porosity by higher PTFE fraction in the MPL. This also explains why these two MEAs show slightly lower DMFC performance than MEA-3 in both quick-scan polarization and steady-current discharge as shown in Figs. 2 and 4, respectively. There is an average 10–20 mV voltage drop at 150 mA/cm^2 when MPL thickness doubles or PTFE loading increases, as shown in Table 1.

The α values of the two MEAs were measured at different current densities and displayed in Fig. 5. For MEAs with single MPL, double MPL, and higher PTFE content, there is no significant difference in α at each current density and in fact, some of the data points overlap. At 150 mA/cm^2 α values of MEA-4 and MEA-5 are 0.312 and 0.302, respectively, compared to 0.335 of MEA-3 as shown in Table 1. The MEAs with thicker MPL and higher PTFE content in the MPLs show almost the same α value, and the α value difference between the two cases is only 0.01, within the experimental errors. Enhancement of MPL surface hydrophobicity by increasing PTFE loading would be limited, since 60 wt.% PTFE is probably sufficient to coat surfaces of carbon particles constituting the MPL. Further increase of PTFE content would only thicken the coating layer without changing the surface hydrophobicity appreciably [24]. Furthermore, 2 M methanol solution more easily wets a substrate than pure water at 60 °C because of its lower surface energy. Therefore, reducing α by using higher PTFE content in MPL has limited potential. It would be challenging to find more hydrophobic materials than PTFE for a methanol–water solution.

5. Conclusions

Effect of anode MPL on water transport in DMFCs has been studied experimentally and theoretically. Both single cell and anode polarization tests indicate that methanol transport in the anode is negligibly influenced by a hydrophobic MPL, but is inhibited by a hydrophilic MPL, due to reduced porosity by ionomer hydration and swelling. Constant-current discharge reveals that the MEA with hydrophobic MPL displays much smaller voltage fluctuation than the hydrophilic one, probably due to the diminished cathode flooding resulting from its higher water back-transport to the anode. MEA-3 with a hydrophobic MPL is verified to have α values several times smaller than those without MPL or with hydrophilic MPL at various current densities. Theoretical calculations indicated that hydrophobic MPL has a high entry liquid pressure, and thus renders the anode more gaseous with a very small liquid saturation. The present study clearly suggests that hydrophobic anode MPL is critical to reducing α while achieving high performance. The calculation also shows that improving MPL hydrophobicity is more effective for α-reduction than increasing the MPL thickness, although experiments have not shown effective reduction of α value. Future work is needed to understand and control water transport between the anode and cathode and to develop highly hydrophobic diffusion media.

Acknowledgement

Financial support of this work by ECEC industrial sponsors is gratefully acknowledged.

References

[1] A.S. Aricò, S. Srinivasan, V. Antonucci, Fuel Cells 1 (2001) 133.
[2] G.Q. Lu, F.Q. Liu, C.Y. Wang, Electrochem. Solid-State Lett. 8 (2005) A1.
[3] F.Q. Liu, G.Q. Lu, C.Y. Wang, J. Electrochem. Soc. 153 (2006) A543.
[4] X. Ren, S. Gottesfeld, J. Electrochem. Soc. A87 (2001) 148.
[5] C.Y. Wang, F.Q. Liu, Proceedings of the 8th Small Fuel Cell Symposium, Washington, DC, April 2006 (Chapter 10).
[6] F.Q. Liu, Ph.D. Thesis, The Pennsylvania State University, University Park, PA, May 2006.
[7] K.Y. Song, H.K. Lee, H.T. Kim, J. Electrochim. Acta 53 (2007) 637.
[8] S. Kang, S.J. Lee, H. Chang, J. Electrochem. Soc. 154 (2007) B1179.
[9] C. Xu, T.S. Zhao, Y.L. He, J. Power Sources 171 (2007) 268.
[10] C. Lim, C.Y. Wang, J. Power Sources 113 (2003) 145.
[11] A. Blum, T. Duvdevani, M. Philosoph, N. Rudoy, E. Peled, J. Power Sources 117 (2003) 22.
[12] X. Ren, F.W. Kovacs, K.J. Shufon, S. Gottesfeld, U.S. Patent Pub. No. US 2004/0209154 A1 (2004).
[13] S.C. Yao, X.D. Tang, C.C. Hsieh, Y. Alyousef, M. Vladimer, G.K. Fedder, C.H. Amon, Energy 31 (2006) 636.
[14] U. Pasaogullari, C.Y. Wang, J. Electrochem. Soc. 151 (2004) A399.
[15] C.Y. Wang, Chem. Rev. 104 (2004) 4727.
[16] C.Y. Wang, P. Cheng, Int. J. Heat Mass Transfer 39 (1996) 3607.
[17] C.Y. Wang, P. Cheng, Adv. Heat Transfer 30 (1997) 93.
[18] F.Q. Liu, C.Y. Wang, J. Electrochem. Soc. 154 (2007) B514.
[19] U. Pasaogullari, C.Y. Wang, Electrochim. Acta 49 (2004) 4359.
[20] W.P. Liu, Ph.D. Thesis, The Pennsylvania State University, University Park, PA, 2005.
[21] C.A. Shaffer, C.Y. Wang, Penn State Electrochemical Engine Center, 2008 (Unpublished work).
[22] C.Y. Wang, in: W. Vielstich, A. Lamm, H.A. Gasteiger (Eds.), Handbook of Fuel Cells—Fundamentals, Technology and Applications, vol. 3, Wiley, Chichester, 2003 (Chapter 29).
[23] X.G. Yang, F.Y. Zhang, A.L. Lubawy, C.Y. Wang, Electrochem. Solid-State Lett. 7 (2004) A408.
[24] C. Lim, C.Y. Wang, Electrochim. Acta 49 (2004) 4149.

Electrochimica Acta 53 (2008) 7357

Contents lists available at ScienceDirect

Electrochimica Acta

journal homepage: www.elsevier.com/locate/electacta

Erratum

Erratum to "Water and methanol crossover in direct methanol fuel cells—Effect of anode diffusion media" [Electrochimica Acta 53 (2008) 5517–5522]

Fuqiang Liu[1], Chao-Yang Wang*

Departments of Materials Science and Engineering, and Mechanical and Nuclear Engineering, and Electrochemical Engine Center (ECEC), The Pennsylvania State University, University Park, PA 16802, United States

The publisher regrets that this article was published with errors in Table 1. The first row of Table 1 should be changed from "MEA-1 C paper w/ anode MPL(aMPL)" to "MEA-1 C paper w/o anode MPL(aMPL)".

The corrected Table 1 for this article is reprinted below:

Table 1
Electrochemical performance parameters of MEAs using different anode diffusion media

Sample	Anode diffusion medium	HFR ($\Omega\,cm^2$)	MeOH crossover at open circuit, $I_{c,oc}$ (mA/cm^2)	Average cell voltage at 150 mA/cm^2 (V)	α-Value at 150 mA/cm^2
MEA-1	C paper w/o anode MPL(aMPL)	0.190	257	0.379	1.153
MEA-2	C paper w/ hydrophilic aMPL	0.183	223	0.328	1.743
MEA-3	C paper w/ hydrophobic aMPL	0.212	242	0.398	0.335
MEA-4	C paper w/ two-layer MPL	0.218	240	0.387	0.312
MEA-5	Carbon paper w/ higher PTFE fraction (60%) in aMPL	0.191	237	0.379	0.302

DOI of original article:10.1016/j.electacta.2008.03.011.
* Corresponding author. Tel.: +1 814 863 4762; fax: +1 814 863 4848.
E-mail address: cxw31@psu.edu (C.-Y. Wang).
[1] Present address: United Technologies Research Center, East Hartford, CT 06108, United States.

0013-4686/$ – see front matter
doi:10.1016/j.electacta.2008.05.015